Inhibition of RIPK1 prevents keratinocyte cell death and reduces skin inflammation in type 1–mediated chronic inflammatory skin diseases

Manja Jargosch, PhD,[a,b] Sophia Wasserer, MD,[a] Jessica Eigemann,[c] Theresa Raunegger,[a] Nils Kurzen,[c] Danping Ding-Pfennigdorff, PhD,[d] Eckart Bartnik, PhD,[d] Carsten B. Schmidt-Weber, PhD,[b] Tilo Biedermann, MD,[a] Stefanie Eyerich, PhD,[b,e,f] Kilian Eyerich, MD, PhD,[f] Peter Florian, PhD,[d,g] Matthias Herrmann, PhD,[d] Joachim Saas, PhD,[d] and Felix Lauffer, MD, PhD[c] *Munich, Neuherberg, Frankfurt am Main, Freiburg, and Ingelheim, Germany*

Background: Type 1–mediated chronic inflammatory skin diseases affect skin, hair, nails, and mucosa and dramatically impact patients' quality of life. The 2 most prominent examples are lichen planus (LP) and cutaneous lupus erythematosus (CLE). Various cell death pathways are activated in both diseases, including apoptosis and necroptosis. RIPK1 is a key regulator of programmed cell death and thus represents a potential new target for treatment of these diseases.

Objective: We sought to determine the impact of RIPK1 on cell death and inflammation in LP and CLE.

Methods: RNA sequencing of inflammatory skin diseases (n = 179) assessed cell death, hypothermia, and inflammatory markers affected by eclitasertib, a novel RIPK1 inhibitor, in human cells, murine TNF-α-induced systemic inflammatory response syndrome model, reconstructed human epidermis, and *ex vivo* skin biopsy culture.

Results: Markers of apoptosis (*CASPASE8*) and necroptosis (*RIPK3*, *MLKL*) are upregulated in LP and CLE. Eclitasertib restored body temperature when orally administered 15 minutes after TNF-α injection in the murine systemic inflammatory response syndrome model. RIPK1 inhibition prevented keratinocyte cell death; normalized epidermal architecture; and decreased release of IL-1α, IL-1β, TNF-α, and CCL20 in reconstructed human epidermis on stimulation with LP and CLE T-cell supernatant. *Ex vivo* culture of LP and CLE biopsy specimens with eclitasertib reduced expression of disease-specific genes and downregulated pathways associated with inflammation.

Conclusions: Inhibition of RIPK1 targets 2 major pathogenic events in LP and CLE: epidermal cell death and type 1–mediated skin inflammation. (J Allergy Clin Immunol 2026;■■■:■■■-■■■.)

Key words: *Lichen planus, cutaneous lupus erythematosus, targeted therapy, necroptosis, cell death, RIPK1, eclitasertib*

Chronic inflammatory skin diseases (ISDs) are increasingly frequent in Western countries and severely impact patients' quality of life. Although there have been great achievements for the 2 most common ISDs, psoriasis and atopic dermatitis (AD), the majority of ISDs lack safe and effective treatments.[1] Lichen planus (LP) and cutaneous lupus erythematosus (CLE) are the 2 most prominent examples of type 1–mediated ISDs. The estimated prevalence of LP is about 1%.[2] LP has a wide clinical spectrum, classically manifesting as itchy papules at the extremities and white net-shaped and erosive plaques at the oral and genital mucosa. However, there are also generalized, exanthematic LP subtypes as well as LP leading to nail dystrophy and scarring alopecia. Likewise, CLE has a wide clinical spectrum and can either solely affect the skin or be a sign of SLE. The 4 most common subtypes of SLE are acute, subacute, chronic discoid, and tumid types. Similar to LP, CLE can affect the mucosa and cause scarring alopecia. Both LP and CLE are usually treated with nonspecific immunosuppressants, such as topical and systemic glucocorticosteroids, antimalarials, methotrexate, or retinoids. However, these strategies often fail to achieve sufficient long-term disease control or need to be discontinued due to side effects.[3] So far, no targeted treatment for LP or CLE has been approved worldwide.

Histologically, LP and CLE are characterized by a lymphocytic infiltrate close to the epidermis, which causes cell death of basal keratinocytes. This immune reaction is named interface dermatitis (ID) and resembles a pattern of immune-epithelial interaction, which can also be found in graft-versus-host disease, dermatomyositis, and viral infections and as a side effect of immune checkpoint inhibitors used for cancer treatment.[4-7] In our previous work, we discovered that LP and CLE share a common gene regulation pattern, which comprises genes belonging to type 1 immunity (*TBX21*, *STAT1*, *IFNG*, *IRF1*, *IRF2*, *IRF3*, *IL12*, or *IL12R*). Thus, based on the shared type 1–dominant immune response, these diseases are grouped as type 1–mediated ISDs. Considering the strong activation of T-cell pathways in our network analysis, T cells were isolated from lesional skin biopsy specimens for in-depth analysis. Intracellular cytokine staining revealed a high frequency of IFN-γ- and TNF-α-positive cells

From [a]the Department of Dermatology and Allergy, Technical University of Munich, Munich; [b]Center of Allergy and Environment (ZAUM), Technical University of Munich and Helmholtz Zentrum Munich, Munich and Neuherberg, Member of the German Center of Lung Research (DZL); [c]the Department of Dermatology and Allergy, LMU Hospital, Munich; [d]Immunology and Inflammation Therapeutic Area, Sanofi R&D, Sanofi, Frankfurt am Main; [e]Institute for Immunodeficiency, Center for Chronic Immunodeficiency, Medical Center-University of Freiburg, Faculty of Medicine, University of Freiburg, Freiburg; [f]the Department of Dermatology and Venereology, University Medical Center Freiburg, Freiburg; and [g]Global Animal Health Research, Boehringer Ingelheim Vetmedica GmbH, Ingelheim.

Received for publication July 18, 2025; revised January 21, 2026; accepted for publication February 4, 2026.

Corresponding author: Felix Lauffer, MD, PhD, Department of Dermatology and Allergy, LMU Hospital, Frauenlobstr 9–11, 80337 Munich, Germany. E-mail: felix.lauffer@med.uni-muenchen.de.

0091-6749

https://doi.org/10.1016/j.jaci.2026.02.006

Abbreviations used
AD: Atopic dermatitis
CLE: Cutaneous lupus erythematosus
DMSO: Dimethyl sulfoxide
IC_{50}: Half maximal inhibitory concentration
ID: Interface dermatitis
ISD: Inflammatory skin disease
JAK: Janus kinase
LP: Lichen planus
RNA-Seq: RNA sequencing
SIRS: Systemic immune response syndrome
TCS: T-cell supernatant

in both lupus erythematosus and CLE,[8] a finding that was confirmed by Shao et al[9] demonstrating the importance of the IFN-γ/JAK2 pathway for the pathogenesis of LP. In addition, we demonstrated that type 1 cytokines cause apoptosis and necroptosis of basal keratinocytes.[8] In the latter case, IFN-γ and TNF-α initiate cell death by activating the RIPK1 signaling pathway. On activation of TNFR1, RIPK1 is released from complex I and activated by autophosphorylation at serine 166, which serves as a biomarker for RIPK1 kinase–dependent pathologies.[10,11] Activated RIPK1 can initiate the formation of 2 distinct prodeath signaling complexes: IIa and IIb. Complex IIa includes the assembly of RIPK1, FADD, and caspase 8 and promotes RIPK1-dependent apoptosis, whereas impaired caspase-8 activity shifts the assembly toward the necroptotic complex IIb, which includes RIPK1, FADD, caspase 8, RIPK3, and MLKL. Here, activated RIPK1 phosphorylates RIPK3, which in turn activates and phosphorylates MLKL. This results in the generation of pores in the outer cell membrane, as well as cell bursting and uncontrolled release of intracellular components—a process known as necroptosis.[11-14] In contrast to apoptosis, necroptosis is a strong inflammatory process and accelerates local inflammation. RIPK1 is centrally involved in both forms of cell death, apoptosis and necroptosis, and therefore represents an interesting new therapeutic target. However, there is no approved RIPK1 inhibitor for the use in humans, so far.

Therefore, we investigated the therapeutic potential of eclitasertib, a novel inhibitor of RIPK1, in murine and human models of type 1 inflammation. We demonstrated that caspase 8, RIPK3, and MLKL were highly upregulated in CLE and LP and that blocking RIPK1 kinase activity prevented keratinocyte cell death and release of proinflammatory cytokines *in vitro*. Furthermore, RIPK1 inhibition normalized body temperature in a murine TNF-α-dependent systemic immune response syndrome (SIRS) model and significantly downregulated disease-specific genes and pathways in human LP and CLE skin biopsy specimens. Thus, targeting RIPK1 kinase activity may represent a novel therapeutic approach for the treatment of type 1–mediated ISDs.

METHODS

Sex as a biological variable

Our study examined tissue samples and cells from male and female patients, and similar findings are reported for both sexes. Detailed patient characteristics are listed in Tables E1, E2, and E3 in this article's Online Repository available at www.jacionline.org.

Study cohort and ethic compliance

Human skin samples were obtained from the Biederstein Biobank and collected in accordance with the Declaration of Helsinki protocol and local ethics committee Klinikum Rechts der Isar (44/16S and 5590/12). All patients gave their written informed consent. To establish a definitive diagnosis, both clinical and histologic evaluations were performed by independent dermatologists and dermatopathologists. Under local anesthesia, 6-mm punch biopsies of lesional and nonlesional skin were collected. Biopsy specimens were divided into 3 parts: 1 part was fixed in 4% formalin for histology, 1 part was collected in RNAlater stabilization solution (Qiagen, Venlo, The Netherlands) at −80°C until RNA preparation, and 1 part was directly used for isolation of lesional T cells. For human lesional skin biopsy cultures, separated 6-mm punch biopsies were used. Table E1 lists characteristics of patients in the bulk RNA sequencing (RNA-Seq) cohort of LP (n = 30), CLE (n = 11), AD (n = 48), and psoriasis (n = 90) skin lesions. Table E2 lists characteristics of patients in the RIPK1 inhibitor treatment cohort of human lesional skin biopsy specimens of LP (n = 5) and CLE (n = 2). *In vivo* mouse studies conducted at Sanofi in Frankfurt am Main, Germany, were approved by the government of Hessia (FH-1036). Male C57BL/6 mice (weight 20-27 g) were obtained from Charles River Laboratories (Wilmington, Mass).

Bulk RNA-Seq analysis of skin biopsy specimens and keratinocyte skin equivalents

Gene expression data for LP (n = 30), CLE (n = 11), AD (n = 48), and psoriasis (n = 90) were derived from a previously published study cohort.[15] Patients' characteristics are listed in Table E1. RNA-Seq libraries were generated using the TruSeq Stranded Total RNA kit (Illumina, San Diego, Calif) according to the manufacturer's high sample protocol. Samples were sequenced on an Illumina HiSeq 4000 as paired-end with a read length of 2× 150 bp and an average output of 40 Mio reads per sample and end. Sequence alignment was performed using STAR aligner with human genome reference hg38 (https://github.com/alexdobin/STAR). RNA-Seq count data were normalized by the median of ratios method, as implemented in the DESeq2 protocol, and then transformed using the variance stabilizing transformation from the Bioconductor package DESeq2 (https://bioconductor.org/packages/release/bioc/html/DESeq2.html). Gene set enrichment analysis was conducted in R using the clusterProfiler package (https://bioconductor.org/packages/release/bioc/html/clusterProfiler.html), org.Hs.eg.db (https://bioconductor.org/packages/release/data/annotation/html/org.Hs.eg.db.html), and the Gene Ontology database (https://geneontology.org/).

RIPK1 inhibitor

The RIPK1 inhibitor eclitasertib (SAR443122, PubChem CID 130298939), also known as DNL758 (Denali Therapeutics), was provided by Sanofi (Paris, France).[16-18] It was dissolved in dimethyl sulfoxide (DMSO) to provide a 10-mM stock solution. For animal experiments, RIPK1 inhibitors were dosed in 0.5% methylcellulose, 0.1% Tween 80 (Sigma-Aldrich, Burlington,

Mass). The concentrations used are indicated in the following sections.

Biochemical RIPK1-autophosphorylation assay (ADP-Glo assay)

The catalytic activity of RIPK1 was determined based on the conversion of ATP to ADP due to autophosphorylation using an ADP-Glo kinase kit (catalog no. V9104; Promega, Madison, Wis). For this, 2 μL of recombinant HIS-GST-TEV-human RIPK1 (amino acids 1-375) (Evotec, Abingdon, United Kingdom) or HIS-GST-TEV-mouse RIPK1 (amino acids 1-378) (Proteros Biostructures GmbH, Martinsried, Germany) fusion proteins (end concentration 4 μg/mL and 42 μg/mL, respectively) were incubated with 2 μL of RIPK1 inhibitor eclitasertib (end concentration 33-0.00168 μM) for 30 minutes at room temperature. Subsequently, 2 μL of ATP (ADP Glo kit, end concentration 50 μM) was added. After incubation for 4 hours at room temperature, 5 μL of Promega ADP-Glo reagent I was added to quench the reaction and deplete unconsumed ATP. After another incubation period of 30 minutes, 10 μL of Promega ADP-Glo detection reagent II was added resulting in conversion of ADP to ATP, which generates a light reaction between luciferase and luciferin. Luminescence was quantified after 30 minutes with a PHERAstar FS microplate reader (BMG Labtech, Ortenberg, Germany). The RIPK1 fusion proteins, ATP, and compounds were diluted in assay buffer consisting of 50 mM HEPES pH 7.5, 50 mM NaCl, 30 mM $MgCl_2$, 1 mM dithiothreitol, 0.02% Tween 20, and 0.02% BSA. For each concentration response curve, the half maximal inhibitory concentration (IC_{50}) values were estimated using the fitted 4-parameter logistic model, and geometric mean values of IC_{50} with 95% CI were calculated.

Culture and necroptosis assay of U937 and L929 cells

Human monocytic leukemia U937 cells (DSMZ no. ACC 5) were cultured in RPMI 1640 medium (72400-021, Gibco/Thermo Fisher, Waltham, Mass) without phenol red and supplemented with 10% FBS at 37°C and 5% CO_2. Mouse NCTC clone 929 (L cell, L929) cells (CLL1, ATCC) were cultured in DMEM/F12 + 15 mM HEPES + L-glutamine medium (11330-032, Gibco/Thermo Fisher) supplemented with 10% heat inactivated FBS (F4135, Sigma-Aldrich), 100 U/mL penicillin, and 100 μg/mL streptomycin at 37°C and 5% CO_2. The cellular potency of eclitasertib was tested in a human cellular necroptosis assay. For this, 50,000 U937 cells or 10,000 L929 cells (cultivated overnight) were stimulated for 18 to 24 hours with 50 ng/mL TNF-α (H8916, Sigma-Aldrich), 25 μM Z-VAD-FMK (V116, Sigma-Aldrich) with or without RIPK1 inhibitor eclitasertib (0.07-10,000 nM for U937 cells or 0.038-10,000 nM for L929 cells). Subsequently, cell viability was determined using the CellTiter 96 AQueous Non-Radioactive Cell Proliferation Assay (G5421, Promega) (see section Cell viability assay).

Culture and necroptosis assay of human PBMCs

PBMCs were isolated from fresh human whole blood using standard methods and cultured in RPMI 1640 GlutaMAX (61870-010, Gibco/Thermo Fisher) supplemented with 10% heat inactivated FBS (F4135, Sigma) at 37°C and 5% CO_2. Before cell death induction with 15 ng/mL LPS Ultrapure (tlrl-3pelps, InvivoGen, San Diego, Calif), PBMCs were pretreated for 30 minutes with 20 μM zVAD-fmk (ALX-260-020-M005, Enzo, Farmingdale, NY) and RIPK1 inhibitor eclitasertib (0.026-100 nM). After 3 hours of incubation at 37°C, cell culture supernatants were collected and stored at −20°C before assaying. IL-1β was quantified using a human IL-1β uncoated ELISA (88-7261-88, Invitrogen, Carlsbad, Calif) according to the manufacturer's instructions.

Culture and necroptosis assay of primary human keratinocytes

Primary human keratinocytes were obtained from healthy donors by suction blister as reported previously[19]; donor characteristics are listed in Table E3. Epidermal keratinocytes were cultured in keratinocyte medium (DermaLife Basal Medium supplemented with DermaLife K LifeFactors Kit, LL-0007, Lifeline Cell Technology, San Diego, Calif) at 37°C and 5% CO_2, and second to third passages were used. At 70% to 80% of confluence, keratinocytes were preincubated for 1 hour with RIPK1 inhibitor eclitasertib (100 nM or as indicated) followed by stimulation with rhIFN-γ (100 ng/mL or as indicated, 285-IF-100/CF, R&D Systems, Minneapolis, Minn) and rhTNF-α (100 ng/mL or as indicated, 210_TA/CF, R&D Systems) in the presence of zVAD (20 μM, 60332, Cell Signaling Technology, Danvers, Mass), SMAC mimetics (1 μM, B-9135, LC Laboratories, Woburn, Mass), and the RIPK1 inhibitor for 24 hours in keratinocyte medium without hydrocortisone.

Three-dimensional skin equivalents

Three-dimensional keratinocyte skin equivalents were generated as described previously.[20] Briefly, 300,000 primary human keratinocytes were seeded in 500 μL of keratinocyte medium with 1.5 mM of $CaCl_2$ in the insert and placed in a well containing the same medium. After 2 days, keratinocytes were exposed to the air-liquid interface, and medium in the surrounding well was supplemented with 50 μg/mL vitamin C. At 9 days after airlift, the skin equivalents were pretreated for 1 hour with RIPK1 inhibitor eclitasertib (100 nM) followed by stimulation with a supernatant mix of lesional T cells from patients in the LP and CLE cohorts (1:10 diluted) in the presence of zVAD (20 μM, 60332, Cell Signaling Technology), SMAC mimetic (1 μM, B-9135, LC Laboratories), and the RIPK1 inhibitor for 72 hours. Afterward, membranes of the fixated skin equivalents were cut out with a scalpel, divided into 2 pieces, formalin fixed, and embedded in paraffin.

Isolation of lesional T cells from LP and CLE skin biopsy specimens and production of supernatant

Primary human lesional T cells were isolated from freshly obtained skin biopsy specimens of patients with LP (n = 5) and CLE (n = 3) (see Table E1 for patient characteristics) by emigration toward an IL-2 gradient followed by expansion with α-CD3/α-CD28 stimulation as described previously.[8,21] Supernatants of expanded lesional T cells were generated by 3-day stimulation with 0.75 μg/mL α-CD3 (precoated, BD Biosciences, Franklin Lakes, NJ) and 0.75 μg/mL soluble α-CD28 (BD Biosciences).

A mixture of all 8 lesional supernatants at equimolar ratio was used for stimulation of 3D keratinocyte skin equivalents. Concentrations of key cytokines in the supernatant mix of lesional T cells were determined by a multiplex ELISA (Bio-Rad Laboratories, Hercules, Calif) (Table E4 in the Online Repository at www.jacionline.org).

Human lesional skin biopsy cultures

Under local anesthesia, 4- to 6-mm punch biopsy specimens of lesional skin of patients with LP (n = 5) and CLE (n = 2) were obtained. Patients' characteristics are listed in Tables E1, E2, and E3. Biopsy specimens were divided into 2 parts with 1 part treated with the RIPK1 inhibitor eclitasertib (1 μM) 1 part without eclitasertib as a control sample for 4 hours in T-cell media (RPMI 1640 medium with 1% human serum, 0.1 mM nonessential amino acids, 2 mM L-glutamine, 1 mM sodium pyruvate, and 100 U/mL penicillin/streptomycin). After stimulation, biopsy specimens were stored in RNAlater solution at −80° C until RNA preparation.

TNF-α-driven SIRS model

A TNF-α-driven SIRS model was created as described before.[22] Briefly, male C57BL/6 mice (n = 6 per group) were injected into the tail vain with a volume of 125 μL per 25 g mouse of either vehicle (15% polyethylene glycol 200, 8.4% DMSO, 0.6% NaCl) or a mixture of murine TNF-α (0.3 mg/kg) and zVAD (6.7 mg/kg) prepared in vehicle. No TNF-α/zVAD was administered to the vehicle group. At 15 minutes after induction of hypothermia by application of TNF-α/zVAD mix, animals were orally dosed with RIPK1 inhibitor or GSK′963 (AOBIUS, AOB9775, Batch 6064M, Gloucester, Mass). This time (15 minutes) was chosen to ensure sufficient time for intestinal passage and absorption as well as systemic distribution. Body temperature was monitored every hour using radiofrequency identification technology with IPTT-300 transponders (Bio Medic Data Systems, Seaford, Del) that were injected subcutaneously 2 to 3 days before initiation of the experiment.

Cell viability assay

Cell viability of cultured cells was determined using CellTiter 96 AQueous Non-Radioactive Cell Proliferation Assay according to the manufacturer's instructions. MTS/PMS reagent was used 1:6 diluted in corresponding cell culture media and incubated for 1 hour (primary keratinocytes) or 4 hours (U937 and L929 cells). Afterward, supernatants were analyzed by ELISA at 490 nm minus 700 nm as reference. For keratinocytes, the percentage of cell viability to control stimulation zVAD and SMAC mimetic (100%) was calculated. For U937 and L292 cells, the percentage inhibition of induced necroptotic cell death was calculated as percentage of the maximal inhibition value obtained in the absence of the inducer TNF-α and zVAD. For dose response experiments (primary keratinocytes, U937, L292 cells), an IC_{50} value with 95% CI was calculated with an implemented 4-parameter logistic model.

Multiplex ELISA

Cell-free supernatants derived from keratinocyte stimulation experiments or lesional T-cell supernatants (TCSs) from patients with LP and CLE were analyzed for 27 cytokines, chemokines, and growth factors using the Bio-Plex Pro Human Cytokine 27-plex Assay (Bio-Rad Laboratories) according to the manufacturer's recommendation.

Histology of skin samples and keratinocyte skin equivalents

Fixated skin tissue or keratinocyte skin equivalents were embedded in paraffin. Then 5-μm sections were cut and dewaxed at 65°C for 20 minutes. After rehydration, sections were stained with hematoxylin and eosin using standard methods. High-resolution images (20×) were obtained with an EVOS microscope (Thermo Fisher Scientific, Waltham, Mass).

RNA preparation, cDNA synthesis, and quantitative PCR

RNA was isolated using QIAzol Lysis Reagent (Qiagen) and miRNeasy Mini Kit (Qiagen) according to the manufacturer's protocol. mRNA was transcribed into cDNA with Applied Biosystems High Capacity cDNA Reverse Transcription Kit (Thermo Fisher Scientific). Gene expression was measured on an Applied Biosystems ViiA7 Real-Time PCR system (Thermo Fisher Scientific) using Fast Start Universal SYBRGreen Master Rox (Roche). Primers were ordered from Metabion (http://www.metabion.com) and are listed in Table E5 (in the Online Repository at www.jacionline.org). Data are shown as relative gene expression to untreated sample using the $2^{-\Delta\Delta Ct}$ method.

Western blot

Keratinocytes were lysed in radioimmunoprecipitation assay lysis buffer (Santa Cruz) supplemented with 1 mM sodium orthovanadate, 2 mM phenylmethylsulfonyl fluoride, and proteinase inhibitor cocktail (1:70) according to the manufacturer's instructions. Equal protein concentrations—determined by BCA protein assay—were resolved by SDS-PAGE using Bolt 4-12% Bis-TrisPlus Gels and analyzed by Western blot using enhanced chemiluminescence. The following antibodies were used for staining: rbαhpRIPK1 (Ser166) (65746, 1:1,000 in BSA, Cell Signaling Technology), mαhβ-Actin (A2228, 1:10,000 in milk, Sigma-Aldrich), and αmHRP (115-035-166, 1:10,000 in milk, Jackson ImmunoResearch, West Grove, Pa).

Statistical analysis

Data were analyzed using GraphPad Prism 6 or 10 and visualized as mean ± SEM. Comparison of disease or treatment groups was performed as indicated in figure legends. Significance levels were defined as $P < .05$, $P < .01$, $P < .001$, and $P < .0001$.

RESULTS

RIPK1 gene expression is upregulated in LP and CLE and correlates to the degree of ID

ID is a histologic hallmark of CLE and LP (Fig 1, *A*). To determine the impact of RIPK1 for the generation of ID, we analyzed the expression of *RIPK1*, *RIPK3*, and *MLKL* in LP and CLE as well as AD and psoriasis skin biopsy specimens compared with intraindividual nonlesional skin. Although gene expression of *MLKL* and *RIPK3* was significantly upregulated in lesional skin

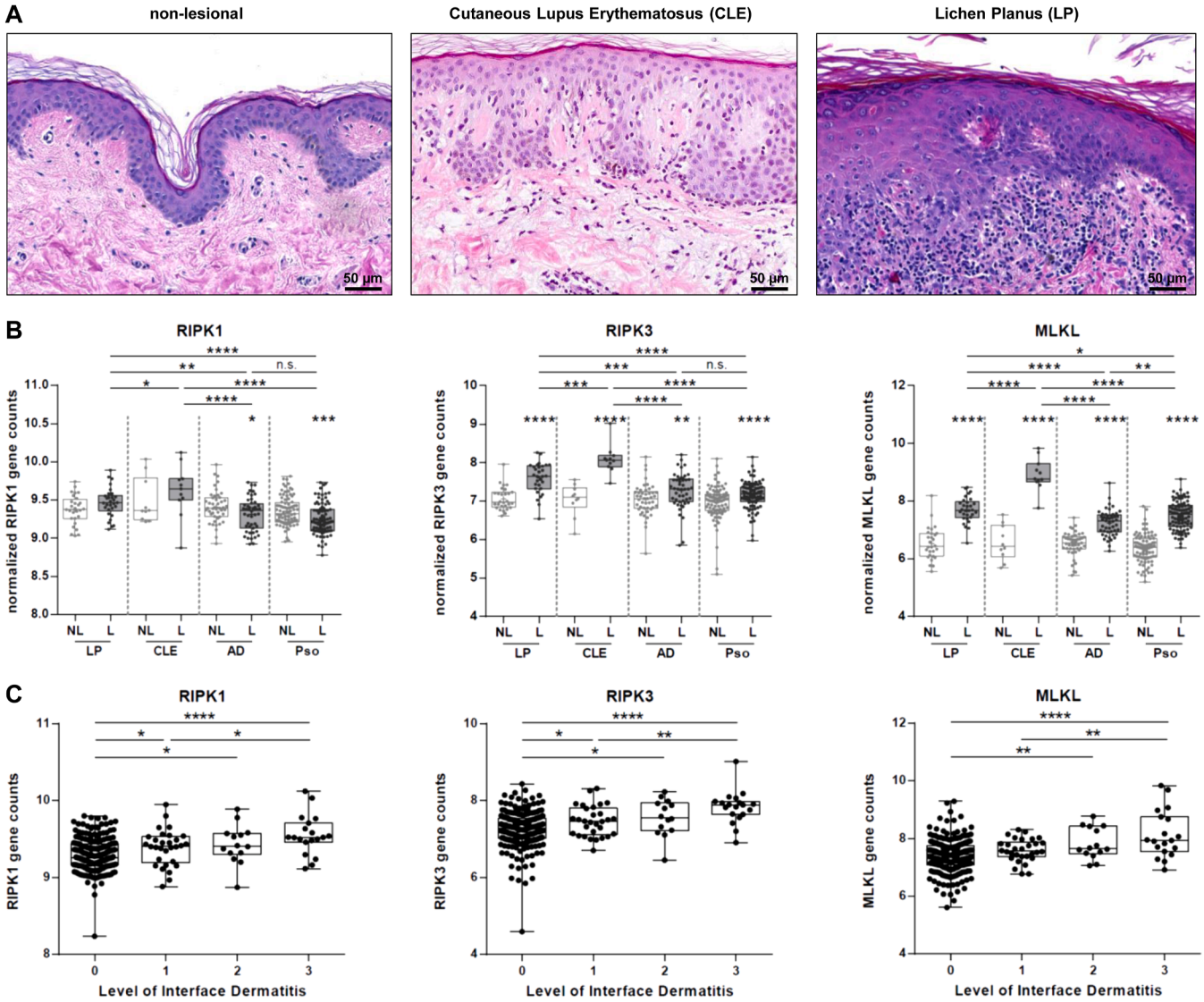

FIG 1. RIPK1, RIPK3, and MLKL are significantly upregulated in lesional skin of patients with LP and CLE and are associated with ID. **(A)** Representative histologic hematoxylin and eosin staining of nonlesional and lesional skin from a patient with CLE and a patient with LP. Scale bar = 50 µm. **(B)** Normalized gene counts of *RIPK1*, *RIPK3*, and *MLKL* in nonlesional and lesional skin of patients with LP (n = 30), CLE (n = 11), AD (n = 48), and psoriasis (n = 90) patients. Differences between the lesional and nonlesional group were analyzed with an unpaired *t* test with Welch's correction. Comparison of patient groups was performed using 1-way ANOVA (uncorrected Fisher's least significant difference). **(C)** Correlation of normalized gene counts for *RIPK1*, *RIPK3*, and *MLKL* to the level of ID in patients with ISD (n = 274) with level 0 (no ID), 1 (mild ID), 2 (moderate ID), and 3 (severe ID). Comparison of ID groups was performed using 1-way ANOVA test (uncorrected Fisher's least significant difference). **P* < .05, ***P* < .01, ****P* < .001, *****P* < .0001. *L*, Lesional; *NL*, nonlesional; *Pso*, psoriasis.

of all 4 diseases (*MLKL*: $P < .0001$ for all; *RIPK3*: $P < .0001$ for LP and CLE; $P = .0140$ for AD; $P = .0035$ for psoriasis), *RIPK1* was significantly higher in lesional LP and CLE than in AD and psoriasis (Fig 1, *B*). Immunofluorescence confirmed enhanced phosphorylated RIPK1, RIPK3, and MLKL expression in the epidermis of LP lesions (Fig E1 in the Online Repository at www.jacionline.org). Next, we assessed the association between ID severity and the gene expression of *RIPK1*, *RIPK3*, and *MLKL*. For this, ID was rated by a dermatopathologist on a scale of 0 (no ID), 1 (mild ID), 2 (moderate ID), and 3 (severe ID) considering the strength of the inflammatory infiltrate and the extent of epidermal cell death. Here, we found a positive correlation between the degree of ID and gene counts of *RIPK1* ($r = 0.98$, $P = .0157$), *RIPK3* ($r = 0.98$, $P = .0163$), and *MLKL* ($r = 0.99$, $P = .0071$) (Fig 1, *C*). To determine activation of further programmed cell death pathways, we analyzed the expression of genes related to apoptosis, ferroptosis and pyroptosis. Only caspase 8 was significantly upregulated in lesional skin of LP and CLE biopsy specimens, whereas markers of classical apoptosis (*BCL2, CASPASE9*), ferroptosis (*GPX4*, *PTGS2*), and pyroptosis

(*GSDMA*, *GSDMB*) were not elevated (Fig E2 in the Online Repository at www.jacionline.org). Of note, caspase 8 is necessary for RIPK1-dependent apoptosis by directly cleaving caspase 3 without activation of caspase 9, indicating that RIPK1-dependent apoptosis and necroptosis are activated in LP and CLE.

Eclitasertib is a potent and selective RIPK1 inhibitor

To further evaluate the role of RIPK1 in LP and CLE, we used the novel RIPK1 inhibitor eclitasertib (Fig 2, *A*). To confirm specificity of eclitasertib, we first performed an ADP-Glo kinase activity assay. Here, ATP to ADP conversion as a result of RIPK1 autophosphorylation was assessed using His-GST-TEV human or murine RIPK1 fusion proteins. Increasing doses of eclitasertib led to a full inhibition of RIPK1 autophosphorylation with an IC_{50} of 8.7 nM (95% CI 5.6-13.4 nM) for human RIPK1 and 144 nM (95% CI 93-223 nM) for murine RIPK1 (Fig 2, *B*). Next, we investigated functional activity in a necroptosis assay with human U937 and murine L929 cells. Here, necroptosis was induced by TNF-α stimulation in the presence of Pan-caspase inhibitor zVAD. Eclitasertib efficiently inhibited necroptosis with an IC_{50} of 4.1 nM (95% CI 2.4-7.2 nM) in human cells and 3.7 μM (95% CI 1.2-11.3 μM) in murine cells (Fig 2, *C* and *D*). To confirm effects in primary human cells, we tested the activity of eclitasertib in human PBMCs stimulated with LPS and zVAD. In line with the previous results, eclitasertib efficiently blocked IL-1β release in a dose-dependent manner (IC_{50} 2.1 nM [1.3-3.4 nM]) (Fig 2, *E*). Next, we tested the effects of eclitasertib on primary human keratinocytes. First, we assessed the impact of different cytokines and Toll-like receptor ligands on inducing keratinocyte necroptosis. Only the combination of TNF-α and IFN-γ significantly impaired keratinocyte viability under necroptotic conditions (Fig E3 in the Online Repository at www.jacionline.org). Then we performed necroptosis assay with human keratinocytes of 3 different donors demonstrating that eclitasertib blocked TNF-α- and IFN-γ-induced necroptosis with an IC_{50} of 0.32 ± 0.21 nM. Using Western blot analysis we confirmed that IFN-γ, TNF-α, and zVAD led to a phosphorylation of the activating S166 site of RIPK1, which was reversed by adding eclitasertib (Fig 2, *G*). Thus, eclitasertib is a potent inhibitor of RIPK1 autophosphorylation preventing cell death, especially necroptosis, in human and murine cell lines and primary human blood and skin cells.

To assess the effects of eclitasertib *in vivo*, we performed a murine TNF-α-driven SIRS model.[22] C57BL/6 mice (n = 6 per group) were injected with either vehicle (15% polyethylene glycol 200, 8.4% DMSO, 0.6% NaCL 0.9%) or a mixture of murine TNF-α (0.3 mg/kg) and zVAD (16.7 mg/kg) into the tail vein. At 15 minutes after induction of hypothermia, animals were orally dosed with eclitasertib or GSK′963, a previously described RIPK1 inhibitor.[23] Body temperature was monitored for up to 5 hours using radiofrequency identification technology with IPTT-300 transponders that were injected subcutaneously 2 to 3 days before initiation of the experiment (Fig 2, *H*). Animals receiving the TNF-α/zVAD mixture rapidly responded with a significant decrease of body temperature within 5 hours from 37.3 ± 0.2°C to 27.9 ± 0.2°C and a temperature change of −9.3 ± 0.3°C (P = .0002) compared with vehicle (−1.9 ± 0.5°C). Oral administration of eclitasertib led to a dose-dependent increase in body temperature change (1 mg/kg: −8.8 ± 0.5°C; 5 mg/kg: −7.6 ± 1.2°C; 15 mg/kg: −3.4 ± 1.3°C, P = .0007 to TNF-α/zVAD) (Fig 2, *I*).

RIPK1 blockade prevents keratinocyte cell death and release of inflammatory cytokines

Based on these findings, we further evaluated the effects of a RIPK1 inhibition in type 1–mediated ISDs. To this end, we performed necroptosis assays with primary human keratinocytes under type 1 inflammatory conditions. Stimulation with IFN-γ, TNF-α, zVAD, and SMAC mimetic (important for full activation of RIPK1 by preventing its ubiquitination) led to 60% cell death of keratinocytes (43.6 ± 7.6% viability), an effect that was fully blocked by RIPK1 inhibition at a concentration of 4 nM (95.1 ± 0.8% viability) or higher (Fig 3, *A*). Furthermore, eclitasertib significantly diminished the release of IL-1β in a dose-dependent manner (P = .0050 for 100 nM) (Fig 3, *B*). Interestingly, RIPK1 inhibition also resulted in significant reduction of IL-1α, IL-1RA, CXCL5, IL-8 (CXCL8), GM-CSF, and CCL20 (Fig 3, *C*).

To test the effects of RIPK1 blockade in a preclinical model of type 1 ISDs, we isolated T cells from LP (n = 5) and CLE (n = 3) skin biopsy specimens and generated TCS by anti-CD3 and anti-CD28 stimulation. LP/CLE-TCS mixed at equal parts contained TNF-α (55,577 pg/mL), GM-CSF (34,800 pg/mL), IL-13 (20,371 pg/mL), and IFN-γ (9,678 pg/mL) (Fig 3, *D*), thereby resembling the natural cytokine composition of type 1 ISDs. In addition, we generated three-dimensional skin equivalents resembling the physiologic layers of the human epidermis. When adding the LP/CLE-TCS under necroptotic conditions, we observed cell swelling and cell death of keratinocytes resulting in an enhanced epidermal thickness (102.0 ± 5.1 μM) compared with controls stimulated with zVAD and SMAC mimetic (61.3 ± 5.4 μM) (Fig 3, *E* and *F*). Blocking RIPK1 by eclitasertib significantly reduced epidermal thickness (80.3 ± 5.1 μM, P < .0001) and restored the normal epidermal architecture (Fig 3, *E* and *F*). In addition, RIPK1 inhibition significantly reduced the release of IL-1RA (48.9 ± 18.0%, P = .0175), TNF-α (70.3 ± 6.3%, P = .0204), and CCL20 (29.1 ± 4.4%, P <.0001) compared with untreated controls, whereas no difference was observed for IL-8 (79.8 ± 9.6%, P = .4757) (Fig 3, *G*). Hence, blocking RIPK1 not only affects cell death of keratinocytes, but also results in markedly decreased proinflammatory cytokines and chemokines.

RIPK1 inhibition downregulates target genes of LP and CLE in human skin biopsy specimens *ex vivo*

To directly examine the effects of RIPK1 inhibition in human tissue samples, we cultured *ex vivo* LP (n = 5) and CLE (n = 2) skin biopsy specimens. Skin biopsy specimens were divided, with one half treated with eclitasertib and the other half cultured in medium for 4 hours (Fig 4, *A*). In contrast to previous experiments, neither additional cytokines nor zVAD or SMAC mimetic were supplemented. Genes specifically upregulated in LP compared with intraindividual nonlesional skin are *IFNG*, *TNF*, *CXCL9*, *CXCL10*, *CXCL11*, *CXCL8*, and *CCL3* (Fig E4, *A*, in the Online Repository at www.jacionline.org). After RIPK1 inhibition, compared with the autologous nontreated controls, we observed a significant downregulation of *IFNG* (60%, P = .0076); *TNF* (60%, P = .0037); *CXCL9*, *CXCL10*, *CXCL11* (57%, 40%, 43%, P = .0128, P = .0024, P = .0045); *CCL3* (62%,

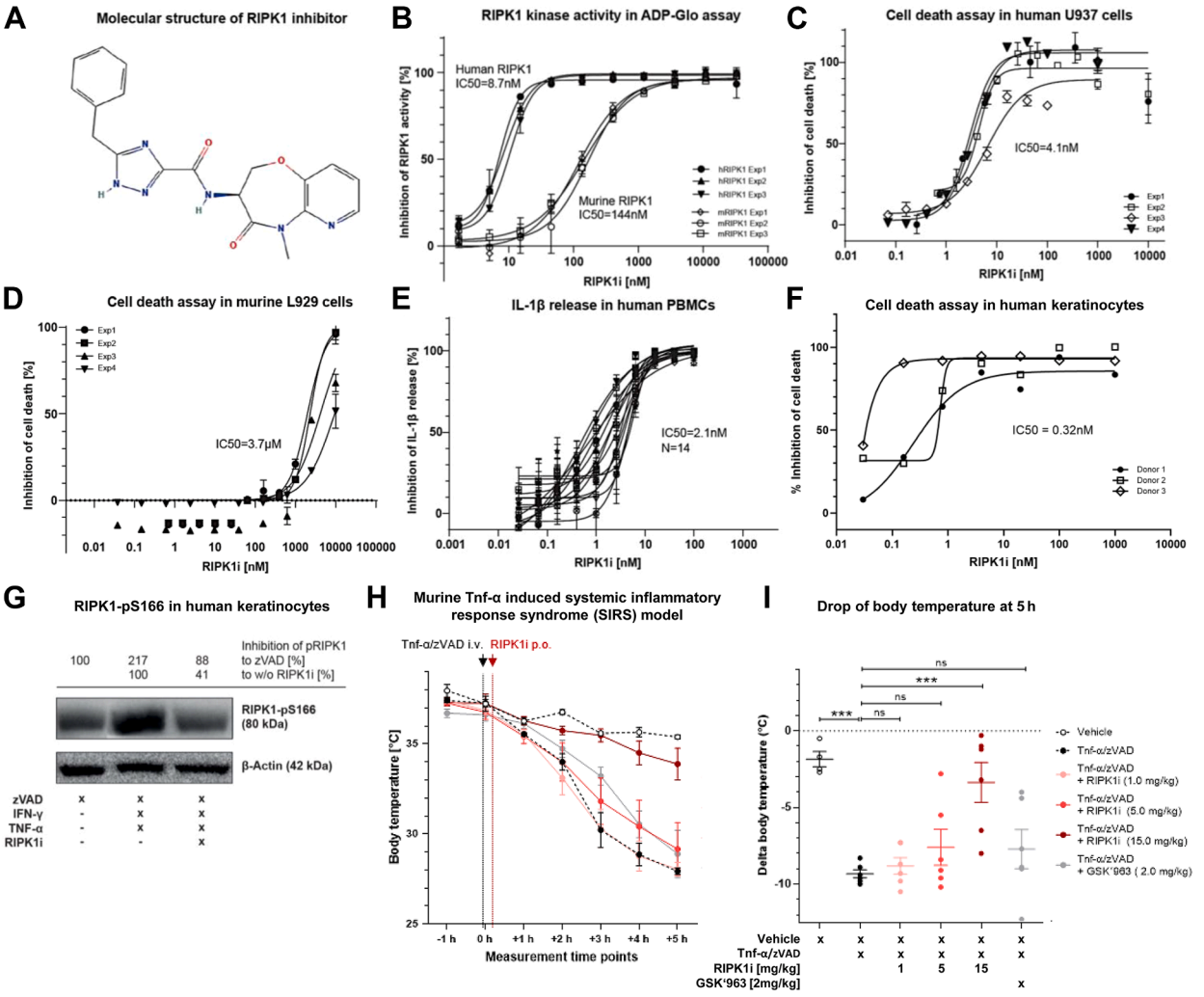

FIG 2. Eclitasertib is a potent and selective RIPK1 inhibitor. **(A)** Molecular structure of RIPK1 inhibitor eclitasertib. **(B)** Inhibition of RIPK1 kinase activity by eclitasertib in the ADP-Glo assay. Dose-dependent inhibition of the catalytic domain kinase activity of human and murine RIPK1 by eclitasertib was determined by monitoring the conversion of ATP to ADP due to autophosphorylation using an ADP-Glo kinase assay (n = 3). Geometric mean IC_{50} values with 95% CI were plotted. **(C** and **D)** Biological *in vitro* activity of eclitasertib in a human U937 *(C)* or murine L929 *(D)* necroptosis assay. Cell viability was determined in U937 or L929 cells 18 to 24 hours after cell death induction with TNF-α (25 ng/mL) + zVAD (25 μM) and treatment with different concentrations (0.07-10,000 nM) of eclitasertib (n = 4). The geometric mean IC_{50} of necroptotic cell death inhibition with 95% CI was determined for eclitasertib. **(E)** Biological *in vitro* activity of eclitasertib in primary human PBMCs measured by IL-1β release. Human PBMCs were stimulated with LPS (15 ng/mL) + zVAD (20 μM) in the presence of different concentrations (0.026-100 nM) of eclitasertib (n = 14). The inhibitory activity of eclitasertib on IL-1β release was determined in cell culture supernatants. The geometric mean IC_{50} inhibitory activity with 95% CI for RIPK1 inhibitor was determined. **(F)** Biological *in vitro* activity of eclitasertib in primary human keratinocyte necroptosis assay. Cell viability was determined in primary human keratinocytes 24 hours after cell death induction with IFN-γ + TNF-α (100 ng/mL) and zVAD (20 μM) + SMAC mimetic (1 μM) and treatment with different concentrations (0.01-10,000 nM) of eclitasertib (n = 3). The geometric mean IC_{50} of necroptotic cell death inhibition was determined for eclitasertib. **(G)** Eclitasertib efficiently blocks S166 phosphorylation of RIPK1. RIPK1-pS166 was detected in Western blot analysis of primary human keratinocytes 6 hours after cell death induction with IFN-γ (10 ng/mL) + TNF-α (10 ng/mL) + zVAD (20 μM) and treatment with RIPK1 inhibitor (100 nM). Relative protein concentrations are calculated to zVAD and to zVAD + IFN-γ + TNF-α without RIPK1 inhibitor and normalized to β-Actin. **(H** and **I)** *In-vivo* testing of eclitasertib by inhibition of hypothermia in a TNF-α-induced SIRS model in mice. C57BL/6 mice (n = 6 per group) received vehicle or murine TNF-α (0.3 mg/kg) and zVAD (16.7 mg/kg) dissolved in vehicle by intravenous injection to induce a systemic inflammatory response (time point = 0 hours). Eclitasertib (1, 5, or 15 mg/kg) or GSK'963 (2 mg/kg) was dosed orally 15 minutes after induction of hypothermia. Body temperature was recorded every hour up to 5 hours and visualized in *(H)*. Drop of body temperature at 5-hour time point after induction of hypothermia was calculated in *(I)*. Comparison of treatment groups was performed with 1-way ANOVA test with Dunnett's multiple correction. ***$P < .001$. *Exp*, Experiment; *i.v.*, intravenous; *ns*, nonsignificant; *p.o.*, peroral; *RIPK1i*, RIPK1 inhibitor eclitasertib.

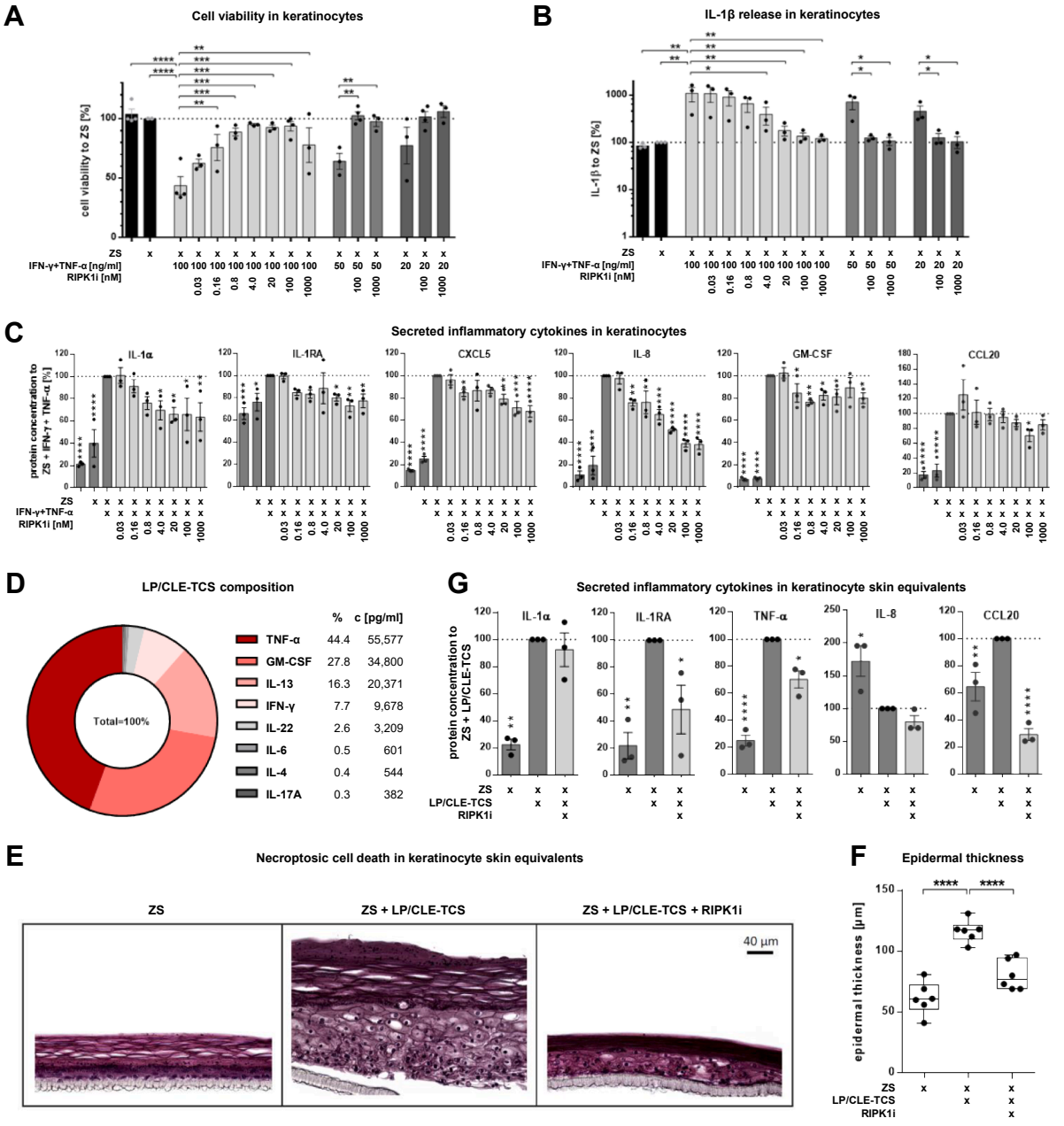

FIG 3. Inhibition of RIPK1 in primary human keratinocytes and keratinocyte skin equivalents diminishes cell death induction, inflammasome activation, and inflammation. **(A-C)** Cell viability *(A)* (n = 4), activity of inflammasome measured by the IL-1β release *(B)* (n = 4), and protein concentrations of secreted inflammatory cytokines *(C)* (n = 3) (100 ng/mL IFN-γ + TNF-α) of primary human keratinocytes 24 hours after cell death induction with IFN-γ + TNF-α and zVAD (20 μM) + SMAC mimetic (1 μM) and treatment with indicated concentrations of RIPK1 inhibitor eclitasertib. **(D)** LP/CLE-TCS composition analyzed by Bio-Plex technique. Lesional TCS mix of 5 LP and 3 CLE donors. T-cell–specific cytokines were visualized as percentages of 100% in total and as absolute concentrations in pg/mL. **(E)** Representative hematoxylin and eosin staining of keratinocyte skin equivalents (n = 3) 72 hours after induction of cell death with LP/CLE-TCS (1:10 diluted) and treatment with eclitasertib (100 nM) under necroptotic conditions with zVAD (20 μM) and SMAC mimetic (1 μM). Scale bar indicates 40 μm. **(F)** Quantification of the epidermal thickness (without stratum corneum) of the keratinocyte skin equivalents in *(E)* under necroptotic conditions (n=3 donors in duplicates). **(G)** Relative concentration of secreted cytokines in the SN of keratinocyte skin equivalent cultures in *(E)* to the stimulated control sample (zVAD and SMAC mimetic + LP/CLE-TCS) without RIPK1 inhibitor treatment (n = 3). Comparison of treatment groups was performed using 1-way ANOVA test (uncorrected Fisher's least significant difference). *$P < 0.05$, **$P < 0.01$, ***$P < 0.001$, ****$P < 0.0001$. *RIPK1i*, RIPK1 inhibitor eclitasertib; *ZS*, zVAD and SMAC mimetic.

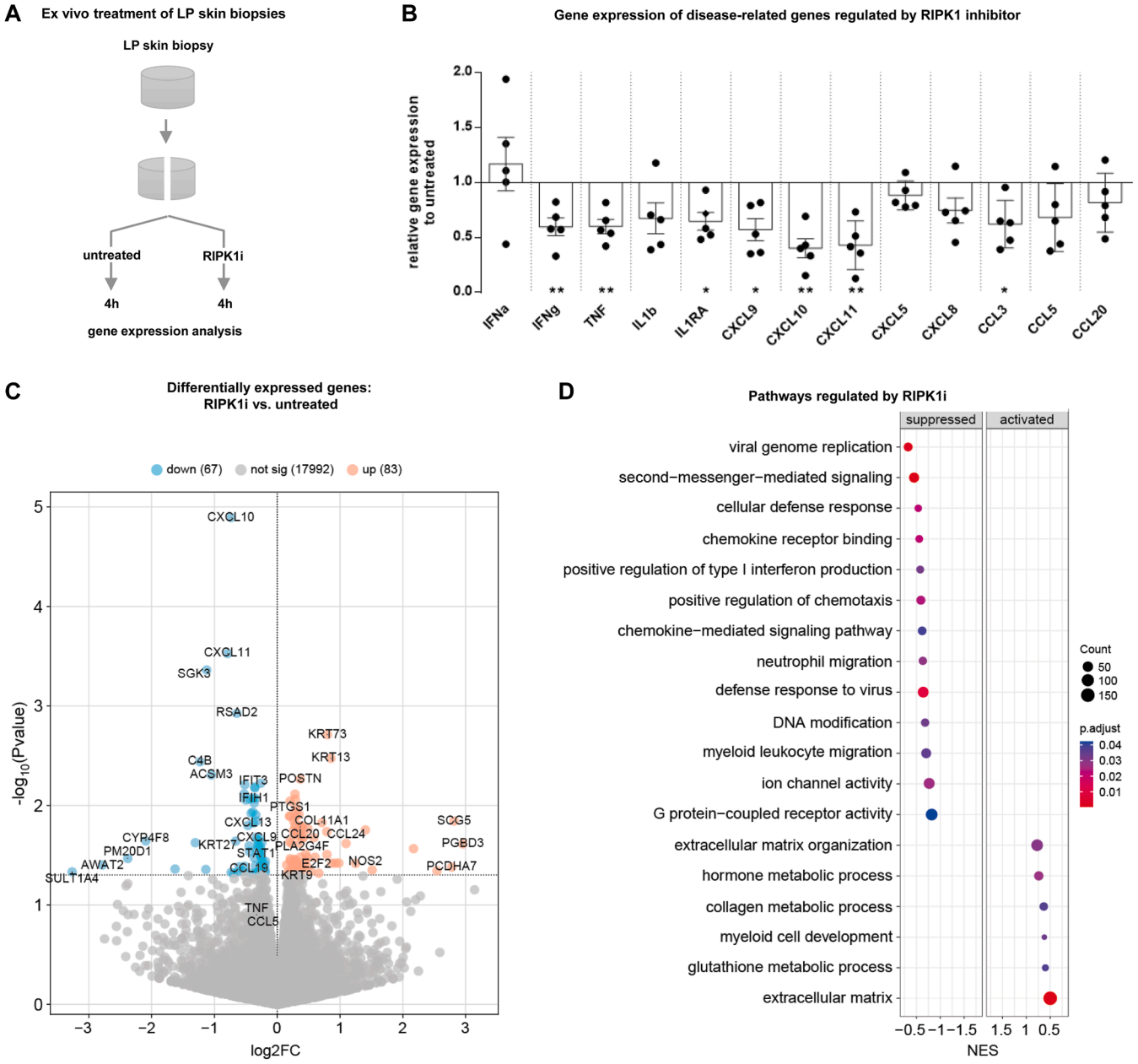

FIG 4. RIPK1 inhibitor eclitasertib suppresses the expression of disease-related genes in cultured lesional skin from patients with LP. *Ex vivo* treatment of LP skin biopsy specimens with eclitasertib (n = 5). **(A)** Experimental setup: 6=mm punch biopsy specimens of lesional skin from patients with LP were collected, divided in 2 parts and incubated for 4 hours with either vehicle or eclitasertib (1 μM), followed by gene expression analysis by quantitative PCR **(B)** and bulk RNA-Seq **(C** and **D)**. *(B)* Gene expression of selected genes in biopsy specimens treated with RIPK1 inhibitor relative to untreated samples measured by quantitative PCR. Comparison of disease groups was performed using unpaired *t* test with Welch's correction. *(C)* Volcano plot of differentially expressed genes ($P < .05$) (n = 150) in biopsy specimens treated with RIPK1 inhibitor compared with untreated specimens. *(D)* Gene set enrichment analysis displaying significantly suppressed and activated pathways by RIPK1 inhibitor treatment in LP skin biopsy specimens. *$P < .05$, **$P < .01$. *FC,* Fold change; *NES,* normalized enrichment score; *RIPK1i,* RIPK1 inhibitor eclitasertib; *sig,* significant.

$P = .0174$); and *IL1RA* (65%, $P = .0123$) (Fig 4, *B*). In line with these results, disease-specific markers (*MX1*, *TLR7*, *IFI27*, and *IL1B*) and necroptosis-associated genes (*MLKL* and *RIPK3*) were reduced by RIPK1 inhibition in CLE skin biopsy specimens (n = 2) (Figs E4, *B*, and E5 in the Online Repository at www.jacionline.org). To validate these findings, we performed bulk RNA-Seq of treated and untreated LP samples. In total, 67 genes were significantly downregulated by eclitasertib; among these,

CXCL9, *CXCL10*, and *CXCL11* ($P = .0001$, $P = -.0003$); *STAT1* ($P = .0235$); and interferon-induced genes such as *IFIT3* and *IFIH1* ($P = .0084$, $P = .0085$) (Fig 4, *C*). Pathway analysis revealed a suppression of several pathways involved in inflammation, such as chemokine binding, cellular defense response, type 1 interferon signaling, and neutrophil migration. Meanwhile, pathways associated with tissue remodeling (collagen metabolic process, extracellular matrix) were activated by RIPK1 inhibition (Fig 4, *D*). In summary, *ex vivo* biopsy treatment with eclitasertib led to a broad downregulation of genes and pathways associated with type 1 inflammation.

DISCUSSION

In this study, we demonstrate that targeting RIPK1 is a promising approach for the treatment of LP and CLE, 2 type 1–mediated ISDs. We observed positive effects of RIPK1 inhibition by eclitasertib on cell death and inflammation in primary human keratinocytes, three-dimensional skin equivalents exposed to LP/CLE-TCS, a murine TNF-α-dependent SIRS model, and *ex vivo* culture of human LP and CLE skin biopsy specimens.

Much progress has been made in understanding and treating ISDs over the last decade. Intense research activities in the most frequent diseases, psoriasis, and AD have already led to numerous new therapeutic options. However, LP and CLE are still treated with broad immunosuppression as there is no targeted therapy available. So far, most therapeutic approaches have aimed at inhibiting immune cell function or blocking immune cell mediators. Shao et al[9] confirmed the importance of IFN-γ for the pathogenesis of LP and proposed JAK2 blockade as a potential new treatment strategy. Indeed, several case reports have demonstrated efficacy of Janus kinase (JAK) inhibition in LP,[24-26] and phase 2 clinical trials using the JAK1/2 inhibitor baricitinib or the TYK2 inhibitor deucravacitinib are ongoing (Clinicaltrials.gov identifiers NCT05188521, NCT06091956, NCT06091956). Baricitinib showed positive effects on skin lesions in SLE; however, the clinical development program was discontinued due to contradictory results of 2 phase III studies.[27,28] Though there might be beneficial effects on skin lesions of type 1–mediated ISDs, JAK inhibition affects several immune functions, and high rates of respiratory infections have been described.[29-31] Furthermore, there are still concerns about serious adverse events during JAK inhibition, such as venous thrombosis or major cardiac events.[32] Therefore, the US Food and Drug Administration[33] has a black box warning on all currently approved JAKs for the treatment of inflammatory diseases, especially for elderly patients.

In contrast, blocking inflammatory cell death does not lead to broad immunosuppression as it can occur only at the site of inflammation. Using SHARPIN-deficient chronic proliferative dermatitis mice (Sharpin$^{cpdm/cpdm}$), which spontaneously develop severe skin and multiorgan inflammation, Laurien et al[10] demonstrated that targeting RIPK1 kinase activity reduces *Tnf*, *Il1b*, *Il6*, *Cxcl3*, and *Ccl3* mRNA and thereby prevents RIPK1-dependent colitis, hepatitis, and cancer as well as skin inflammation. Several drugs blocking necroptosis have been identified in cellular assays.[34-36] However, to our knowledge, there is no necroptosis inhibitor approved for use in humans at the present time, and it is not clear if sole inhibition of necroptosis would be sufficient to reduce inflammation. Our data show that cell death is a central pathogenic event in LP and CLE, as inhibition leads to downregulation of various immune pathways including IFN-γ and TNF-α.

RIPK1 is involved in various forms of cell death, such as RIPK1-dependent apoptosis via complex IIa and necroptosis via the formation of complex IIb. In addition, it has been shown that RIPK1 controls the activation of pyroptosis mediated by gasdermin proteins GSDMD and GSDME via caspase 8 in macrophages and neutrophil granulocytes in the context of *Yersinia* infections.[37] Interestingly, GSDME-mediated pyroptosis also amplifies cutaneous inflammation in psoriasis.[38] In this respect, it can be assumed that several forms of cell death are usually activated in parallel during inflammatory reactions. In line with this, previous data from our research group have shown that keratinocytes stimulated with the supernatant of T cells from CLE and LP skin biopsy specimens show both induction of cleaved caspase 3 as a sign of apoptosis and phosphorylated MLKL as a sign of necroptosis, depending on the dilution of the TCS.[8] Furthermore, cell death–independent proinflammatory effects of RIPK1 and RIPK3 have been reported.[39] In line with our observations in preclinical models of skin inflammation, it has recently been demonstrated that S161 autophosphorylation is also necessary for the induction of skin inflammation in murine models.[40] As RIPK1 is centrally involved in several forms of cell death and inflammation, it represents an ideal target structure for diseases with ID, such as LP and CLE.

Eclitasertib has clinically been evaluated for the treatment of ulcerative colitis, CLE, and severe COVID-19 pneumonia. A phase II study testing eclitasertib in patients with ulcerative colitis is currently recruiting (Clinicaltrials.gov identifier: NCT05588843). In a phase I clinical trial, eclitasertib versus placebo was tested in 68 patients with severe COVID-19 pneumonia. Here, RIPK1 inhibition was well tolerated and showed trends for an earlier improvement of biomarkers (C-reactive protein) and clinical symptoms compared with placebo. However, due to the small sample size, the differences between eclitasertib and placebo were not significant.[41] First results of a proof-of-concept study testing the effects of eclitasertib in CLE have recently been published on clinicaltrials.gov (Clinicaltrials.gov identifier: NCT04781816). In this trial, 78 patients received either eclitasertib or placebo (1:1 randomization). Patients receiving eclitasertib showed a mean Cutaneous Lupus Erythematosus Disease Area and Severity Index score reduction of 42.76% (SE 5.42) at week 12, whereas patients receiving placebo had a 37.05% (SE 5.31) reduction. The percentage of patients with a Physician Global Assessment score of 0 or 1 (free or mild) was 44.7% in the eclitasertib arm and 32.5% in the placebo group. Though this trial demonstrates trends for a better outcome in the eclitasertib arm, the results of this trial need to be evaluated carefully due to the surprisingly high placebo response. Further evaluation of objective measurements such as biomarker substudies are desirable to better estimate the therapeutic potential for RIPK1 inhibition in CLE.

While evaluating the potential for the treatment of ISDs, it is crucial to point out that type 1 ISDs are excellent models for other inflammatory conditions, such as viral infections, antitumor immunity, or COVID-19 pneumonia. Here, IFN-γ and TNF-α are the central cytokines mediating inflammatory cell death and tissue damage, increasing the risk for COVID-19-related mortality.[42] Our findings about type 1–mediated ISDs are useful to develop new treatment strategies targeting inflammatory cell

death in these conditions. In fact, RIPK3 knockout mice showed higher survival and less weight loss compared with wild-type mice after infection with influenza A(H7N9).[43] Apart from viral infections, several autoimmune diseases show involvement of T_H1 immunity and inflammatory cell death. Among them, SLE is the most prominent example, as ID can also be detected in affected kidneys.[44,45] Furthermore, immune checkpoint blockade by anti-CTLA4, anti-PD1, or anti-PDL1 antibodies often results in cutaneous side effects characterized by an ID.[5,46,47] Hence, inhibition of RIPK1 may represent a new approach with various clinical applications.

Our study has several limitations. First, it is a preclinical validation based primarily on *in vitro* experiments with cells and tissue samples from patients. *In vivo* experiments with models that reflect key aspects of the diseases were not performed, as mouse models of LP are not established, and the majority of SLE mouse models rely on autoantibody-induced glomerulonephritis and do not show a skin phenotype.[48] Second, it cannot be ruled out that the effects of RIPK1 inhibition are overestimated or underestimated due to the heterogeneity of human donors. Third, our analyses do not allow any conclusions to be drawn about the safety and efficacy of RIPK1 inhibition in humans. It is therefore essential that further clinical studies are conducted in accordance with high-quality standards to determine the effectiveness and safety of this new therapeutic approach.

In summary, we report that RIPK1 is critically involved in regulating programmed cell death in LP and CLE. RIPK1 inhibition prevents keratinocyte cell death as well as the release of inflammatory mediators and leads to a downregulation of LP/CLE target genes and pathways in human skin biopsy specimens. These data indicate that targeting RIPK1 is a promising approach for the treatment of type 1−mediated ISDs.

Data and materials availability

Datasets related to this article can be found at GEO under the accession number GSE154200, an open-source online data repository hosted at NCBI. All other data are available in the main text or the supplementary materials.

DISCLOSURE STATEMENT

This work was funded by Sanofi (Paris, France) and German Research Foundation (Deutsche Forschungsgemeinschaft) RTG2668 (Project A3, Project-ID: 435874434).

Disclosure of potential conflict of interest: D. Ding-Pfennigdorff, E. Bartnik, M. Herrmann, and J. Saas are Sanofi employees. P. Florian is a past employee of Sanofi and is now employed by Boehringer Ingelheim Vetmedica GmbH. The rest of the authors declare that they have no relevant conflicts of interest.

This study was performed with samples of the Biederstein Biobank of the Technical University of Munich.

Clinical implications: RIPK1 represents a novel target for the treatment of type 1–mediated ISD.

REFERENCES

1. Ujiie H, Rosmarin D, Schon MP, Stander S, Boch K, Metz M, et al. Unmet medical needs in chronic, non-communicable inflammatory skin diseases. Front Med (Lausanne) 2022;9:875492.
2. Le Cleach L, Chosidow O. Clinical practice. Lichen planus. N Engl J Med 2012; 366:723-32.
3. Ioannides D, Vakirlis E, Kemeny L, Marinovic B, Massone C, Murphy R, et al. European S1 guidelines on the management of lichen planus: a cooperation of the European Dermatology Forum with the European Academy of Dermatology and Venereology. J Eur Acad Dermatol Venereol 2020;34:1403-14.
4. Wenzel J, Tuting T. An IFN-associated cytotoxic cellular immune response against viral, self-, or tumor antigens is a common pathogenetic feature in "interface dermatitis". J Invest Dermatol 2008;128:2392-402.
5. Schaberg KB, Novoa RA, Wakelee HA, Kim J, Cheung C, Srinivas S, et al. Immunohistochemical analysis of lichenoid reactions in patients treated with anti-PD-L1 and anti-PD-1 therapy. J Cutan Pathol 2016;43:339-46.
6. Wenzel J, Zahn S, Bieber T, Tuting T. Type I interferon-associated cytotoxic inflammation in cutaneous lupus erythematosus. Arch Dermatol Res 2009;301: 83-6.
7. Yoneda K, Demitsu T, Matsuoka Y, Moriue T, Nakai K, Kusida Y, et al. Subcellular activation site of caspase-3 in apoptotic keratinocytes observed in lichenoid tissue reaction. Br J Dermatol 2008;158:1166-8.
8. Lauffer F, Jargosch M, Krause L, Garzorz-Stark N, Franz R, Roenneberg S, et al. Type I immune response induces keratinocyte necroptosis and is associated with interface dermatitis. J Invest Dermatol 2018;138:1785-94.
9. Shao S, Tsoi LC, Sarkar MK, Xing X, Xue K, Uppala R, et al. IFN-gamma enhances cell-mediated cytotoxicity against keratinocytes via JAK2/STAT1 in lichen planus. Sci Transl Med 2019;11:eaav7561.
10. Laurien L, Nagata M, Schunke H, Delanghe T, Wiederstein JL, Kumari S, et al. Autophosphorylation at serine 166 regulates RIP kinase 1-mediated cell death and inflammation. Nat Commun 2020;11:1747.
11. Mifflin L, Ofengeim D, Yuan J. Receptor-interacting protein kinase 1 (RIPK1) as a therapeutic target. Nat Rev Drug Discov 2020;19:553-71.
12. Linkermann A, Green DR. Necroptosis. N Engl J Med 2014;370:455-65.
13. Belizario J, Vieira-Cordeiro L, Enns S. Necroptotic cell death signaling and execution pathway: lessons from knockout mice. Mediators Inflamm 2015;2015: 128076.
14. Jorgensen I, Rayamajhi M, Miao EA. Programmed cell death as a defence against infection. Nat Rev Immunol 2017;17:151-64.
15. Garzorz-Stark N, Batra R, Lauffer F, Jargosch M, Pilz C, Roenneberg S, et al. Identifying hidden drivers of heterogeneous inflammatory diseases. Posted July 26, 2020. bioRxiv2020.07.25.221309 2020.
16. Chen L, Zhang X, Ou Y, Liu M, Yu D, Song Z, et al. Advances in RIPK1 kinase inhibitors. Front Pharmacol 2022;13:976435.
17. Levente Petro J, Bana P, Linke N, Eszter Szabo J, Katalin Szalai K, Kalomista I, et al. Harnessing dual-mode RIPK1 ligands for cross-species anti-necroptosis inhibitor compounds. Bioorg Med Chem Lett 2024;113:129970.
18. Petro JL, Benyei G, Bana P, Linke N, Horti F, Szabo JE, et al. Design, synthesis and biological evaluation of novel cyclic malonamide derivatives as selective RIPK1 inhibitors. Bioorg Med Chem Lett 2024;100:129643.
19. Garzorz-Stark N, Lauffer F, Krause L, Thomas J, Atenhan A, Franz R, et al. Toll-like receptor 7/8 agonists stimulate plasmacytoid dendritic cells to initiate TH17-deviated acute contact dermatitis in human subjects. J Allergy Clin Immunol 2018; 141:1320-33.e11.
20. Poumay Y, Dupont F, Marcoux S, Leclercq-Smekens M, Herin M, Coquette A. A simple reconstructed human epidermis: preparation of the culture model and utilization in in vitro studies. Arch Dermatol Res 2004;296:203-11.
21. Tsutsumi Y, Odani K, Kaneko Y, Hashizume H, Tachibana M. Cutaneous coinfection of cytomegalovirus and Mycobacterium chelonae accelerated by immunosuppression. Case Rep Pathol 2021;2021:8819560.
22. Duprez L, Takahashi N, Van Hauwermeiren F, Vandendriessche B, Goossens V, Vanden Berghe T, et al. RIP kinase-dependent necrosis drives lethal systemic inflammatory response syndrome. Immunity 2011;35:908-18.
23. Berger SB, Harris P, Nagilla R, Kasparcova V, Hoffman S, Swift B, et al. Characterization of GSK′963: a structurally distinct, potent and selective inhibitor of RIP1 kinase. Cell Death Discov 2015;1:15009.
24. Seiringer P, Lauffer F, Pilz AC, Boehmer D, Biedermann T, Eyerich K. Tofacitinib in hypertrophic lichen planus. Acta Derm Venereol 2020;100: adv00220.
25. Moussa A, Colla T, Morrison B, Sinclair R. Effective treatment of oral lichen planus with the JAK inhibitor baricitinib. Australas J Dermatol 2022;63:276-7.

26. Damsky W, Wang A, Olamiju B, Peterson D, Galan A, King B. Treatment of severe lichen planus with the JAK inhibitor tofacitinib. J Allergy Clin Immunol 2020;145:1708-10.e2.
27. Wallace DJ, Furie RA, Tanaka Y, Kalunian KC, Mosca M, Petri MA, et al. Baricitinib for systemic lupus erythematosus: a double-blind, randomised, placebo-controlled, phase 2 trial. Lancet 2018;392:222-31.
28. News Release. Updates on OLUMIANT® (baricitinib) Phase 3 lupus program and FDA review for atopic dermatitis. Eli Lilly and Company; 2022. Available at: https://investor.lilly.com/news-releases/news-release-details/updates-olumiantr-baricitinib-phase-3-lupus-program-and-fda. Accessed February 10, 2022.
29. Reich K, Kabashima K, Peris K, Silverberg JI, Eichenfield LF, Bieber T, et al. Efficacy and safety of baricitinib combined with topical corticosteroids for treatment of moderate to severe atopic dermatitis: a randomized clinical trial. JAMA Dermatol 2020;156:1333-43.
30. Bieber T, Simpson EL, Silverberg JI, Thaci D, Paul C, Pink AE, et al. Abrocitinib versus placebo or dupilumab for atopic dermatitis. N Engl J Med 2021;384:1101-12.
31. Reich K, Teixeira HD, de Bruin-Weller M, Bieber T, Soong W, Kabashima K, et al. Safety and efficacy of upadacitinib in combination with topical corticosteroids in adolescents and adults with moderate-to-severe atopic dermatitis (AD Up): results from a randomised, double-blind, placebo-controlled, phase 3 trial. Lancet 2021;397:2169-81.
32. Cohen SB, Tanaka Y, Mariette X, Curtis JR, Lee EB, Nash P, et al. Long-term safety of tofacitinib up to 9.5 years: a comprehensive integrated analysis of the rheumatoid arthritis clinical development programme. RMD Open 2020;6:e001395.
33. FDA requires warnings about increased risk of serious heart-related events, cancer, blood clots, and death for JAK inhibitors that treat certain chronic inflammatory conditions. U.S. Food and Drug Administration; 2021. Available at: https://www.fda.gov/drugs/drug-safety-and-availability/fda-requires-warnings-about-increased-risk-serious-heart-related-events-cancer-blood-clots-and-death. Accessed March 7, 2022.
34. Yan B, Liu L, Huang S, Ren Y, Wang H, Yao Z, et al. Discovery of a new class of highly potent necroptosis inhibitors targeting the mixed lineage kinase domain-like protein. Chem Commun (Camb) 2017;53:3637-40.
35. Fauster A, Rebsamen M, Huber KV, Bigenzahn JW, Stukalov A, Lardeau CH, et al. A cellular screen identifies ponatinib and pazopanib as inhibitors of necroptosis. Cell Death Dis 2015;6:e1767.
36. Degterev A, Linkermann A. Generation of small molecules to interfere with regulated necrosis. Cell Mol Life Sci 2016;73:2251-67.
37. Jetton D, Muendlein HI, Connolly WM, Magri Z, Smirnova I, Batorsky R, et al. Non-canonical autophosphorylation of RIPK1 drives timely pyroptosis to control *Yersinia* infection. Cell Rep 2024;43:114641.
38. Li Y, He Y, Yang F, Liang R, Xu W, Li Y, et al. Gasdermin E-mediated keratinocyte pyroptosis participates in the pathogenesis of psoriasis by promoting skin inflammation. Br J Dermatol 2024;191:385-96.
39. Najjar M, Saleh D, Zelic M, Nogusa S, Shah S, Tai A, et al. RIPK1 and RIPK3 kinases promote cell-death-independent inflammation by toll-like receptor 4. Immunity 2016;45:46-59.
40. Koerner L, Li X, Silnov E, Laurien L, Pasparakis M. RIPK1 autophosphorylation at S161 mediates cell death and inflammation. J Exp Med 2025;222:e20250279.
41. Clot PF, Farenc C, Suratt BT, Krahnke T, Tardat A, Florian P, et al. Immunomodulatory and clinical effects of receptor-interacting protein kinase 1 (RIPK1) inhibitor eclitasertib (SAR443122) in patients with severe COVID-19: a phase 1b, randomized, double-blinded, placebo-controlled study. Respir Res 2024;25:107.
42. Karki R, Sharma BR, Tuladhar S, Williams EP, Zalduondo L, Samir P, et al. Synergism of TNF-alpha and IFN-gamma triggers inflammatory cell death, tissue damage, and mortality in SARS-CoV-2 infection and cytokine shock syndromes. Cell 2021;184:149-68.e17.
43. Xu YL, Tang HL, Peng HR, Zhao P, Qi ZT, Wang W. RIP3 deficiency ameliorates inflammatory response in mice infected with influenza H7N9 virus infection. Oncotarget 2017;8:27715-24.
44. Dunlap GS, Billi AC, Xing X, Ma F, Maz MP, Tsoi LC, et al. Single-cell transcriptomics reveals distinct effector profiles of infiltrating T cells in lupus skin and kidney. JCI Insight 2022;7:e156341.
45. Vermi W, Lonardi S, Morassi M, Rossini C, Tardanico R, Venturini M, et al. Cutaneous distribution of plasmacytoid dendritic cells in lupus erythematosus. Selective tropism at the site of epithelial apoptotic damage. Immunobiology 2009;214:877-86.
46. Sibaud V. Dermatologic reactions to immune checkpoint inhibitors: skin toxicities and immunotherapy. Am J Clin Dermatol 2018;19:345-61.
47. Apalla Z, Sibaud V. Immunotherapy-mediated dermatological adverse events: the urgent need for a common, clinically meaningful, management strategy. Support Care Cancer 2020;28:5597-9.
48. Richard ML, Gilkeson G. Mouse models of lupus: what they tell us and what they don't. Lupus Sci Med 2018;5:e000199.